

Crystal transformation and micropore formation during uniaxial drawing of β -form polypropylene film

Feng Chu, Tetsuji Yamaoka and Yoshiharu Kimura*

Department of Polymer Science and Engineering, Kyoto Institute of Technology,
Matsugasaki, Kyoto 606, Japan

(Received 27 September 1994; revised 20 December 1994)

Polypropylene (PP) films with a high content of β crystal were prepared at crystallization temperatures (T_{cr}) of 20 and 110°C and then uniaxially drawn at different temperatures (T_{dr}). The drawn film prepared at $T_{cr} = 20^\circ\text{C}$ had smaller pore volume and average pore radius than the one prepared at $T_{cr} = 110^\circ\text{C}$ under similar drawing conditions ($T_{dr} = 130^\circ\text{C}$, draw ratio = 3.5–4.0). Electron microscopy revealed that most of the pores are formed by plastic deformation of the weak boundaries of lamellar blocks in the β -PP films. During drawing, the unstable β crystals in the film prepared at $T_{cr} = 20^\circ\text{C}$ were easily deformed to undergo crystal transformation of $\beta \rightarrow \alpha$ or $\beta \rightarrow$ smectic without much increasing the pore volume of the film. In contrast, the more stable β crystals in the film prepared at $T_{cr} = 110^\circ\text{C}$ remained in the drawn film, and the micropores were enlarged. These results suggested that crystal transformation and micropore formation in the drawn films can be controlled by changing both T_{cr} and T_{dr} . The static and dynamic mechanical properties of the β -PP films were also measured to analyse the structural differences of samples of β -PP formed at different T_{cr} .

(Keywords: β -form polypropylene; micropore formation; phase transformation)

INTRODUCTION

The preparation of β -form polypropylene (β -PP) with a relative content of β crystal over 90% has recently been accomplished by use of an effective β -nucleator¹. The β -PP is known to have a unique structure and mechanical properties. Of particular interest is that the β crystal is likely to undergo phase transformation during deformation². Usually, it transforms into smectic form at lower temperature, but into α form at higher temperature, so that c -axis-oriented β crystals have never been observed after drawing. The literature³ reported that these phase transformations are progressive processes, in which the β crystals oriented parallel to the tensile axis are more easily deformed than those at a tilt angle with the tensile axis. Because the density of β crystal is lower than that of α crystal, the phase transformation of $\beta \rightarrow \alpha$ induces volume contraction followed by micropore formation. Our previous paper¹ has given a detailed report on the porosity and structure change of β -PP films drawn under various conditions. The porosity of the drawn films increased with increasing crystallization temperature of β -PP and decreasing drawing temperature. This finding suggested that micropore formation is closely related with the local volume contraction induced by the phase transformation of β crystals and the hindered bulk volume contraction due to the stable β crystals. This paper deals with the static and dynamic mechanical properties of the β -PP films and their morphological and

crystallographic changes in the process of drawing, from which the mechanisms of phase transformation and micropore formation induced by the drawing of β -PP are disclosed.

EXPERIMENTAL

Materials

Polypropylene pellets (melt index = 14) blended with 0.1 wt% of a newly developed β -nucleator (NJSTAR) were supplied by New Japan Chemical Co. Ltd (Kyoto)⁴. β -PP films with a thickness of ca. 0.2 mm were prepared by cooling the hot-pressed PP at a defined crystallization temperature (T_{cr}). Their relative content of β crystal was higher than 90% as calculated by the K value¹. Drawing of the β -PP films was carried out as described in the previous paper¹ at a defined drawing temperature (T_{dr}).

Measurements

Wide-angle X-ray diffraction was measured on an X-ray diffractometer equipped with an X-ray generator (Rigaku 4036A1) and a goniometer (Rigaku PMG-A2). The X-rays were generated at 40 kV and 27.5 mA, and Ni-filtered Cu K_α radiation was used. The pore size and pore-size distribution were determined by the mercury intrusion method and the gas adsorption method using Porosimeter-2000 (Carlo Erba Interment, Italy) and Sorptomatic 1900 (Carlo Erba Interment, Italy) instruments, respectively. In the latter method, the amount of nitrogen gas adsorbed on the walls of pores was

* To whom correspondence should be addressed

measured at various pressures, and the pore size and its distribution were calculated from the isothermal adsorption curve by applying the Brunauer–Emmett–Teller (BET) equation⁵. Scanning electron microscopy (SEM) was performed with a JSM 840 microscope for the gold-coated samples. Transmission electron microscopy (TEM) was carried out on a Hitachi H800 transmission electron microscope. The sample was stained with RuO_4 to enhance the image contrast and cut to a thickness of 40–50 nm by use of a microtome. Tensile measurement was performed with a temperature-variable Instron testing machine (model 4206) at a crosshead speed of 30 mm min^{-1} . The dimensions of the specimen between gauges were 20 mm long and 10 mm wide. Dynamic viscoelastic properties were measured with a Rheospectrometer model DVE-V4 (Rheology Co. Ltd, Kyoto). By loading a synthesized strain consisting of 2^n sine waves,

where n is an integer between 0 and 8, the temperature and frequency dispersion curves were obtained by a single-temperature scan (5°C min^{-1}).

RESULTS AND DISCUSSION

Dynamic mechanical properties of β -PP films

As reported previously¹, the films prepared at $T_{\text{cr}} = 20$ and 110°C had a similar content of β crystal (90%) as determined by K value although the β crystals prepared at $T_{\text{cr}} = 110^\circ\text{C}$ were more stable than those prepared at $T_{\text{cr}} = 20^\circ\text{C}$ in terms of the ease of phase transformation. For further characterization of β -PP films the dynamic mechanical properties were measured. Figure 1 shows the typical results obtained at a strain frequency of 8 Hz. Both films showed a similar behaviour below 130°C . In the relaxation region around the melting point, however,

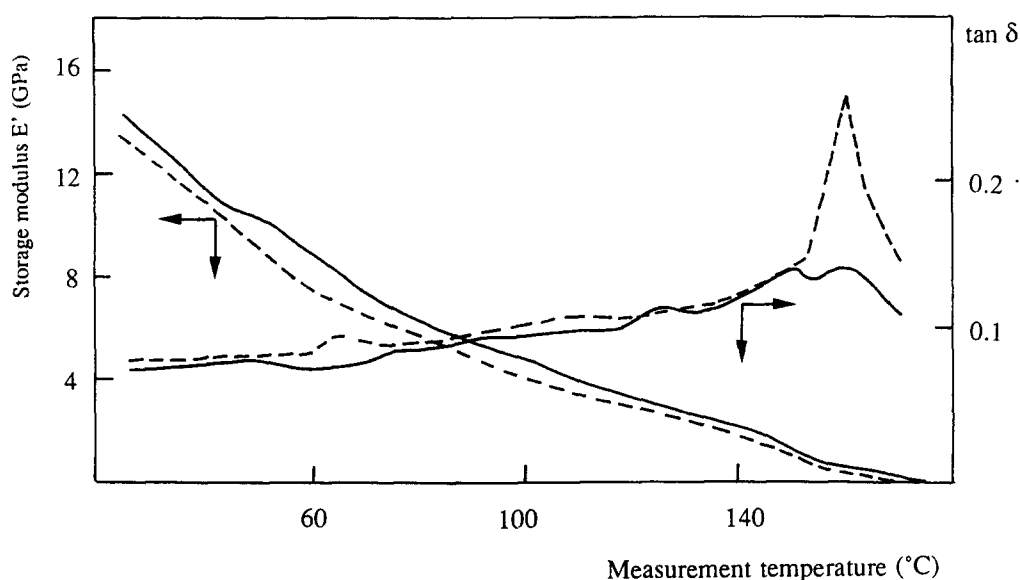


Figure 1 Temperature dependence of dynamic mechanical storage modulus (E') and $\tan \delta$ measured at 8 Hz. The full and broken curves are for films prepared at $T_{\text{cr}} = 20$ and 110°C , respectively

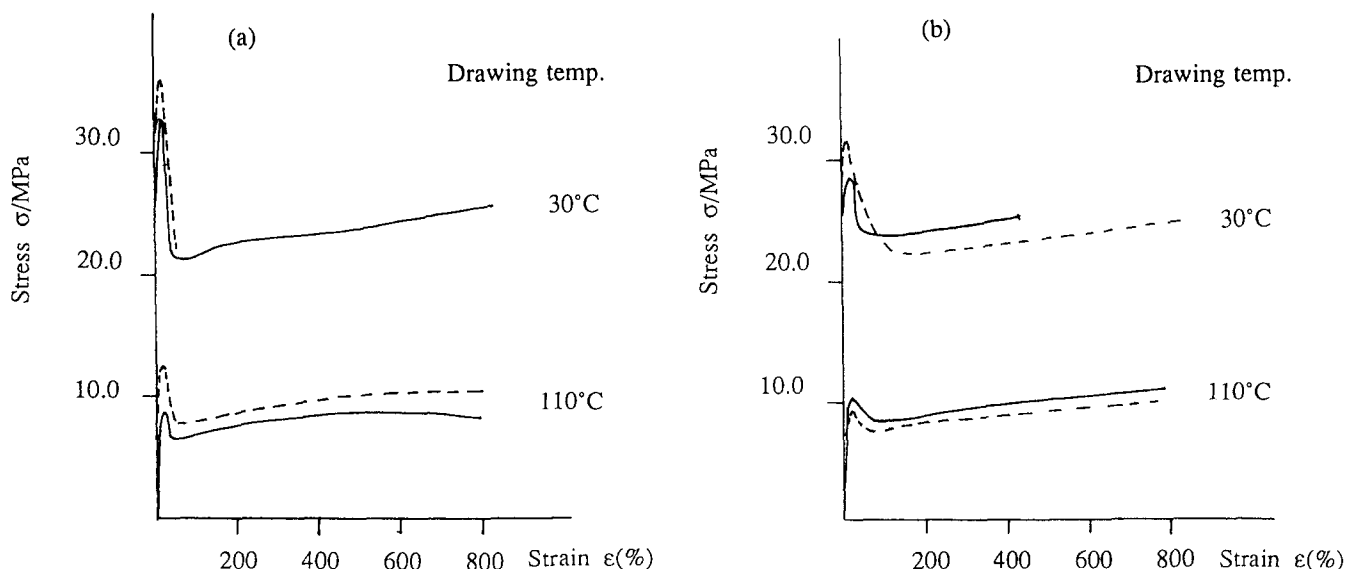


Figure 2 Typical stress–strain curves of (a) α -PP and (b) β -PP films at 30 and 110°C . The full and broken curves are for films prepared at $T_{\text{cr}} = 20$ and 110°C , respectively

the film prepared at $T_{cr} = 20^\circ\text{C}$ showed two peaks in the $\tan\delta$ curve, while that of the film prepared at $T_{cr} = 110^\circ\text{C}$ had a single peak. Since each of these peaks is not accompanied by a critical drop of E' , it may be ascribed to the $\beta \rightarrow \alpha$ crystal transformation, which ought to be driven via partial melting of the β crystals. The two peaks for the former film should be reasonably ascribed to the transformations of the β crystals with different stability. These results indicated that the β crystals transform into the α crystals by a partial melt-recrystallization process near the melting point of the former. At higher strain frequency, the second peak appearing at higher temperature disappeared because the melt-recrystallization process could not keep pace with the strain frequency. It should be noted here that the storage modulus of the β -PP film prepared at $T_{cr} = 20^\circ\text{C}$

became slightly higher than that of the film prepared at $T_{cr} = 110^\circ\text{C}$.

Stretching behaviour of β -PP film

The tensile properties of the β -PP films prepared at $T_{cr} = 20$ and 110°C were measured at a constant drawing rate at 30 and 110°C . Figure 2 shows their typical stress-strain curves as compared with those of α -PP films prepared under similar conditions. Table 1 summarizes the Young's modulus, yield strength and stress at break. It can be seen that β -PP has a lower yield strength than α -PP. In the α -PP, the film prepared at $T_{cr} = 110^\circ\text{C}$ showed a higher yield strength and Young's modulus than the one prepared at $T_{cr} = 20^\circ\text{C}$ at both measurement temperatures. This is quite understandable because the films prepared at higher T_{cr} should have well grown

Table 1 Mechanical behaviours of PP films prepared at various temperatures measured by stress-strain behaviours

Sample	T_{cr} ($^\circ\text{C}$)	T_{dr} ($^\circ\text{C}$)	Yield strength (MPa)	Young's modulus (MPa)	Stress at break (MPa)	Elongation (%)
β -PP	20	30	28.79	1020.0	25.88	611.5
	110		29.38	901.4	26.29	904.5
	20	110	10.27	260.8	9.998	977.5
	110		9.576	192.2	9.479	978.4
α -PP	20	30	33.40	927.6	25.43	977.2
	110		39.10	1246.0	28.01	42.45
	20	110	9.403	182.9	8.913	977.4
	110		12.90	304.0	10.33	977.3

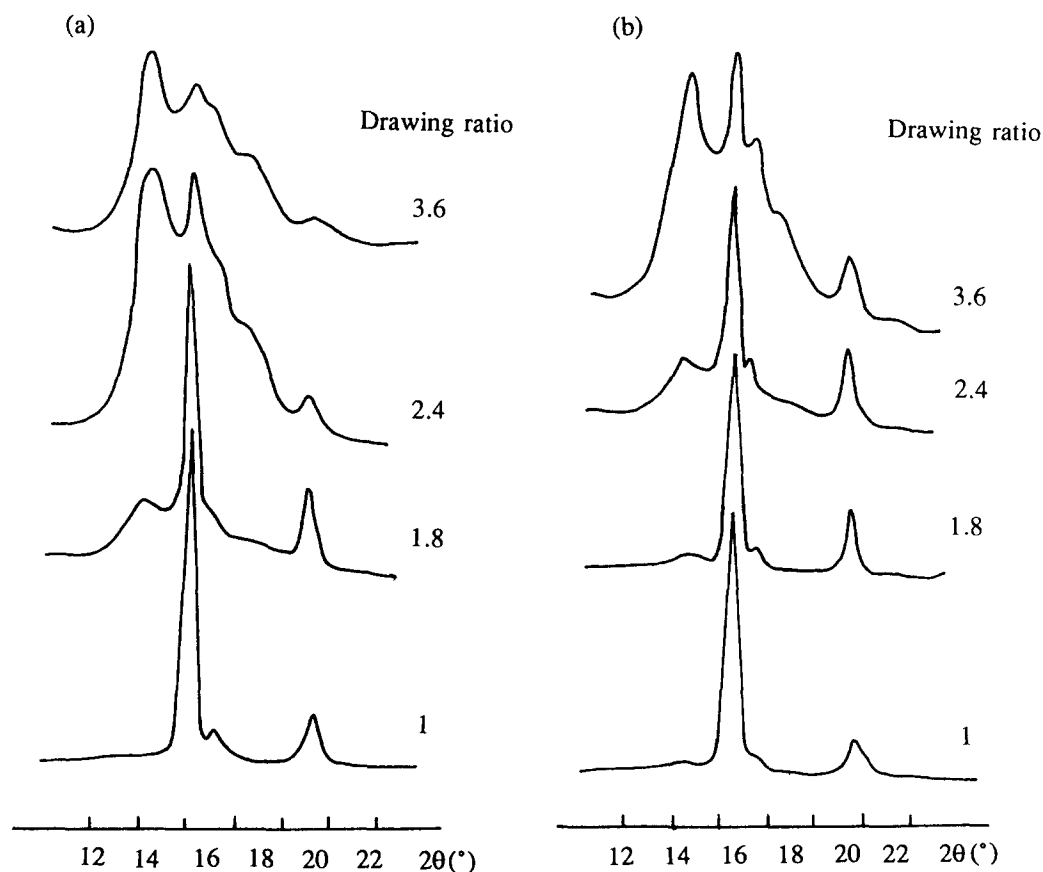


Figure 3 Equatorial X-ray diffractograms of the β -PP films drawn uniaxially at 30°C to the draw ratios indicated; $T_{cr} = 20^\circ\text{C}$ (a) and 110°C (b)

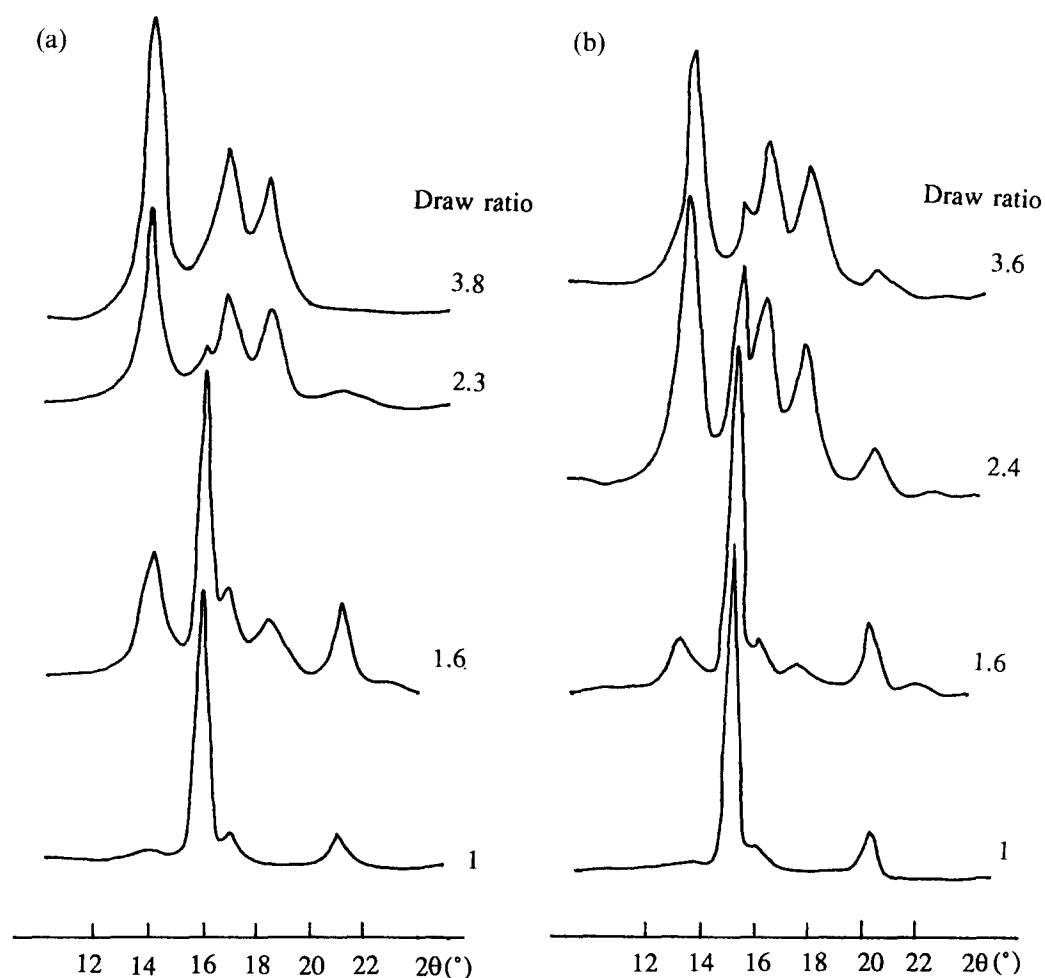


Figure 4 Equatorial X-ray diffractograms of the β -PP films drawn at 110°C up to the draw ratios indicated; $T_{cr} = 20^\circ\text{C}$ (a) and 110°C (b)

Table 2 Pore size, porosity and surface area of drawn β -PP films

T_{cr} ($^\circ\text{C}$)	T_{dr} ($^\circ\text{C}$)	λ	Average pore radius (\AA)		Surface area ($\text{m}^2 \text{g}^{-1}$)		Pore volume ($\text{cm}^3 \text{g}^{-1}$)	
			<i>a</i>	<i>b</i>	<i>a</i>	<i>b</i>	<i>a</i>	<i>b</i>
20	130	4.0	145	95	28.3	5.0	0.179	0.0238
110	130	3.5	561	98	68.9	13.8	0.893	0.0679

^a Measured by mercury intrusion porosimetry

^b Measured by gas (N_2) absorption method

crystallites and spherulites compared with those quenched at lower T_{cr} . In the case of β -PP (see Figure 2b), however, the Young's modulus and the stress after the yield point of the films prepared at $T_{cr} = 110^\circ\text{C}$ were lower than those of the films prepared at $T_{cr} = 20^\circ\text{C}$. This fact is rather unusual in terms of crystallite size of β -PP (*vide infra*). The different stress observed after the yield point can be understood by assuming the $\beta \rightarrow$ smectic or $\beta \rightarrow \alpha$ crystal transformation during the drawing, which was studied by the following X-ray diffraction, porosity measurement and morphology observation.

It is known that the $\beta \rightarrow$ smectic and $\beta \rightarrow \alpha$ transformations proceed from the β crystals whose *c* axes are nearly parallel to the drawing direction, and then to those with the *c* axis at a tilt angle and

perpendicular to the drawing direction³. Therefore, the intensity of the diffraction of β crystals in the equatorial direction can represent the relative content of β crystal remaining in the film at the early stage of drawing. Figure 3 shows the typical equatorial diffractograms for the β -PP films prepared at different T_{cr} and drawn at $T_{dr} = 30^\circ\text{C}$. The draw ratio (λ) was 1.6–3.6, corresponding to the yield point and the further stretching stages of the films. The reflection intensity of the original β crystals decreased with increasing draw ratio, while those ($2\theta = 13\text{--}20^\circ$) of the smectic form increased. It suggested that the β crystals were transformed into the smectic form by drawing at low temperature. This $\beta \rightarrow$ smectic transformation propagated more easily in the film prepared at $T_{cr} = 20^\circ\text{C}$ (Figure 3a) than the one prepared at $T_{cr} = 110^\circ\text{C}$ (Figure 3b). At a draw ratio of

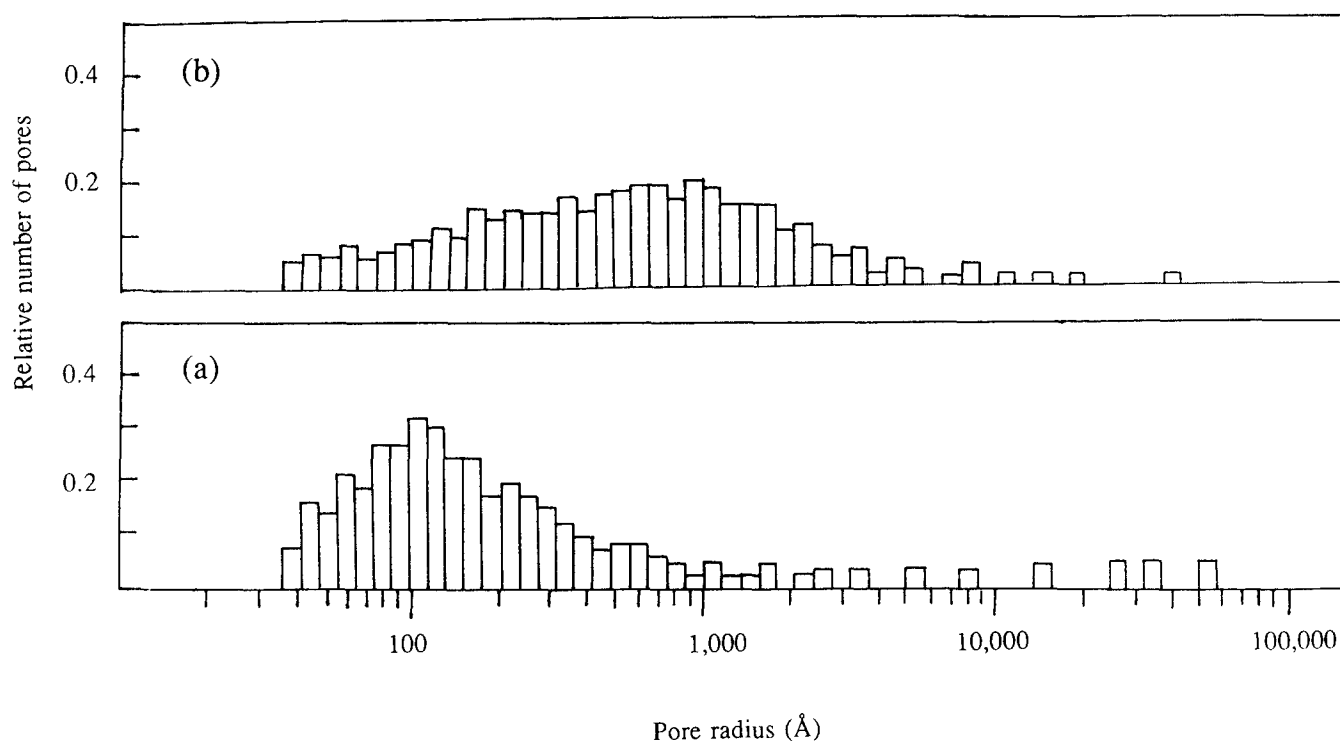


Figure 5 Pore-size distributions of the β -PP films drawn uniaxially at a constant width at 130°C measured by the mercury intrusion method: (a) $T_{cr} = 20^\circ\text{C}$, draw ratio $\lambda = 4.0$; (b) $T_{cr} = 110^\circ\text{C}$, $\lambda = 3.5$

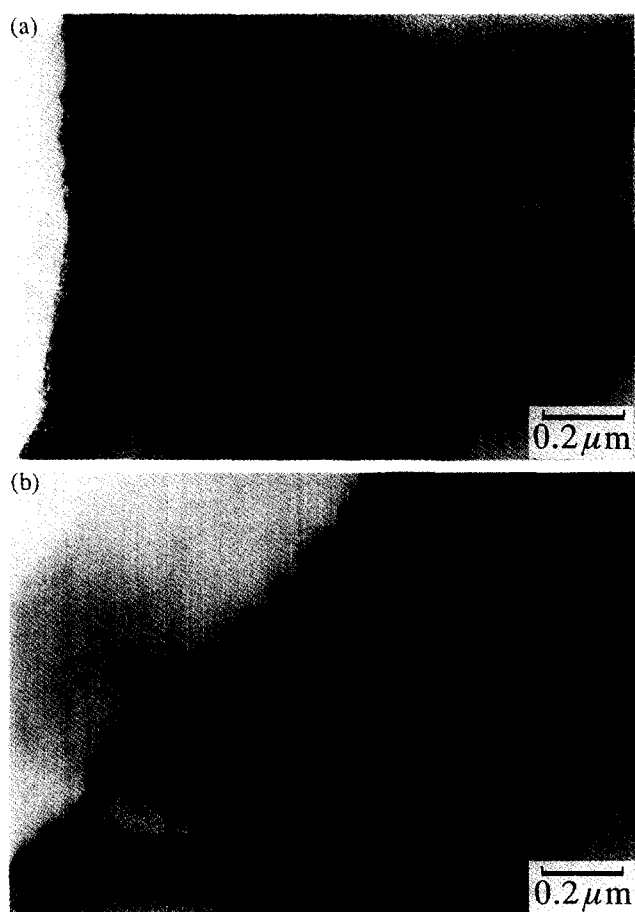


Figure 6 TEM photographs of β -PP films: $T_{cr} = 20^\circ\text{C}$ (a) and 110°C (b)

3.6, a strong β (300) reflection was maintained in the latter, while it almost disappeared in the former.

Figure 4 shows the similar diffractograms for the films drawn at $T_{dr} = 110^\circ\text{C}$. It is known that the $\beta \rightarrow \alpha$ crystal transformation occurred at this drawing temperature. The reflection peaks due to the α crystals were clearly detected at $\lambda = 1.6$, which was just after passing the yield point of both films. The β (300) reflection almost disappeared in the film prepared at $T_{cr} = 20^\circ\text{C}$ and drawn up to $\lambda = 2.3$, while it remained in the film prepared at $T_{cr} = 110^\circ\text{C}$ and drawn up to $\lambda = 3.6$. These results indicate that the β crystals formed at $T_{cr} = 110^\circ\text{C}$ are more resistant to crystal transformation than those formed at $T_{cr} = 20^\circ\text{C}$ and that the crystal transformation is induced around the yield point.

Pore-size distribution of drawn films

Both films prepared at $T_{cr} = 20$ and 110°C were drawn uniaxially with constant width at 130°C . The draw ratio (λ) was 3.5–4.0 where the increase in porosity was to level off¹. The porosity and pore size of the drawn films were measured by the mercury intrusion method as well as by the BET method using nitrogen gas. The results are summarized in Table 2. The data by the mercury intrusion method are for the continuous pores into which mercury can penetrate from the surface. It is known that the film prepared at $T_{cr} = 20^\circ\text{C}$ and drawn up to $\lambda = 4.0$ had a smaller pore volume and a smaller average pore radius than the one prepared at $T_{cr} = 110^\circ\text{C}$ and drawn up to $\lambda = 3.5$. Their typical pore distributions are shown in Figure 5. The former film had a narrower distribution of pore size (mainly distributed around 100 Å) with a number of pores of radii larger than $1\ \mu\text{m}$, while the latter showed a wider pore-size distribution. It is therefore assumed that the difference in porosity was principally attributed to the difference in pore size.

The data by the BET method should be for the micropores of radii less than 100 Å, which are both isolated and connected with each other. It is indicated that the two drawn films had a similar average micropore radius, although the micropore volume and surface area of the film prepared at $T_{cr} = 110^\circ\text{C}$ and drawn up to $\lambda = 3.5$ was slightly larger than those of the drawn film prepared at $T_{cr} = 20^\circ\text{C}$ and drawn up to $\lambda = 4.0$.

Morphology change

Figure 6 shows the TEM photographs of the β -PP films prepared at different T_{cr} . To reveal the real lamellar structure, the RuO_4 staining technique was used in which the dark stained lines should correspond to the amorphous parts between the crystalline lamellae. The lamellar thickness in the film prepared at $T_{cr} = 110^\circ\text{C}$ is ca. 120 Å, which is slightly larger than that in the film prepared at $T_{cr} = 20^\circ\text{C}$ (ca. 100 Å).

Figure 7 shows the SEM photographs of the films drawn uniaxially up to $\lambda = 1.2$ at a constant width: this value of λ corresponds to the yield point of each film. The surface of the film prepared at $T_{cr} = 20^\circ\text{C}$ became uneven with a number of small pores, while that of the film prepared at $T_{cr} = 110^\circ\text{C}$ was wrinkled with many pores. After the surface was etched with a $\text{H}_2\text{SO}_4/\text{H}_3\text{PO}_4$ (2:1) solution containing KMnO_4 (0.7 wt%), it could be

seen that the small pores scattered at places in the former film without a specific structure formed. The latter film, in return, clearly displayed deformed spherulites in which the pores were formed in the boundaries of the spherulite leaves.

Figure 8 shows typical TEM photographs of the β -PP films drawn up to $\lambda = 3.5$. The film prepared at $T_{cr} = 20^\circ\text{C}$ lost the original lamellar structure after drawing to show very thin striations along the drawing direction. These striations are attributed to the fibrillar structure that was formed by unfolding and reordering of molecular chains. As discussed in the previous section, most of the β crystals transformed into α crystals in this stage. The film prepared at $T_{cr} = 110^\circ\text{C}$ and drawn uniaxially showed a conspicuous microfibrillar structure around the pores. The mean width between the microfibrils is about 100 Å. In some parts, the microfibrillar structure was transformed into the well stretched fibrillar structure similar to that shown in Figure 8a by pull-out of the microfibrils (specified by the arrows in Figure 8b). The micropores were formed in the outer boundaries of microfibrils and fibrils. The X-ray diffraction of this film suggested that many of the β crystals had transformed into α crystals by drawing while some (especially, the β crystals with c axis perpendicular to the drawing direction) had still

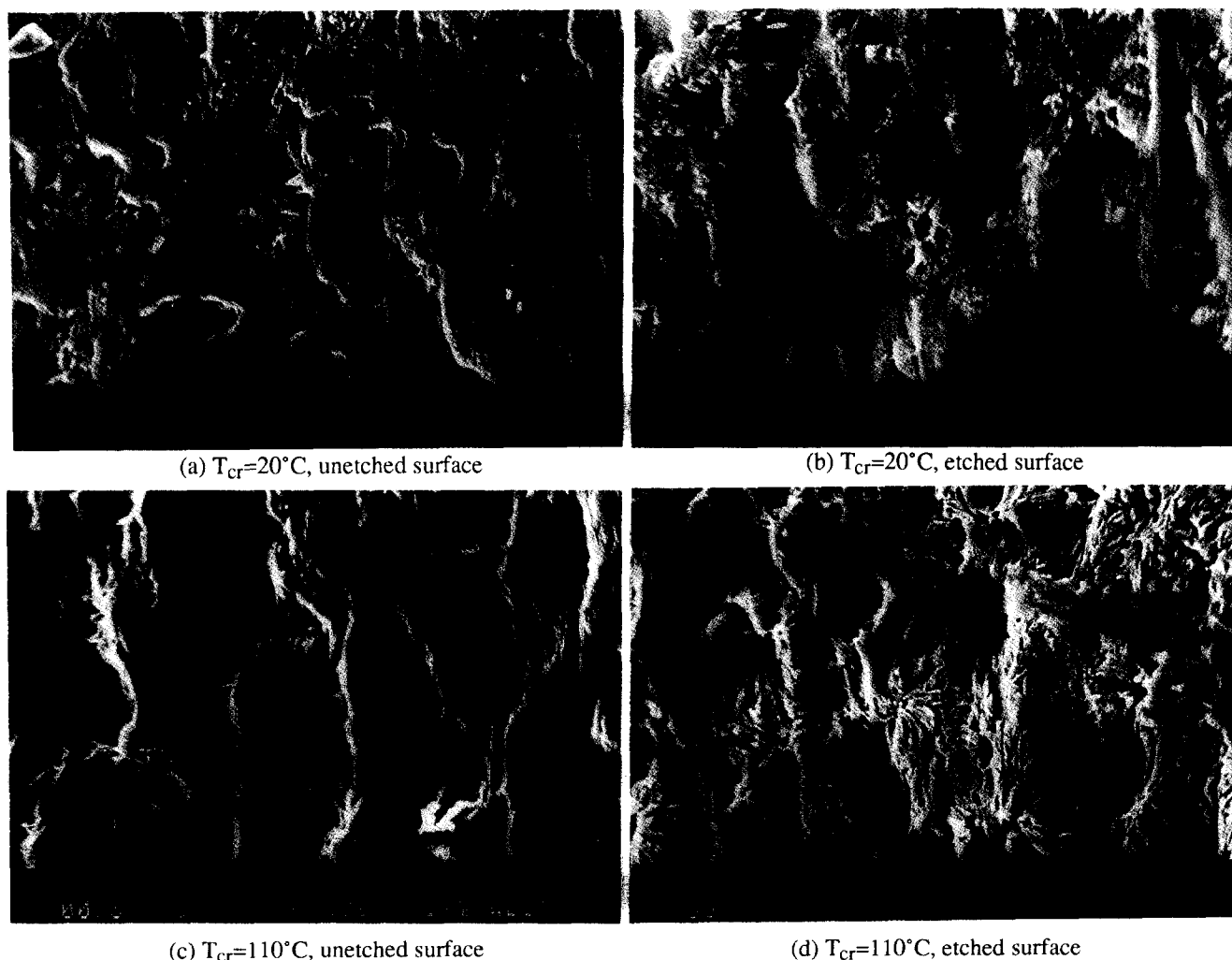


Figure 7 SEM photographs of the films drawn uniaxially up to a draw ratio of $\lambda = 1.2$ at a constant width at 130°C : (a) $T_{cr} = 20^\circ\text{C}$, unetched surface; (b) 20°C , etched; (c) 110°C , unetched; (d) 110°C , etched

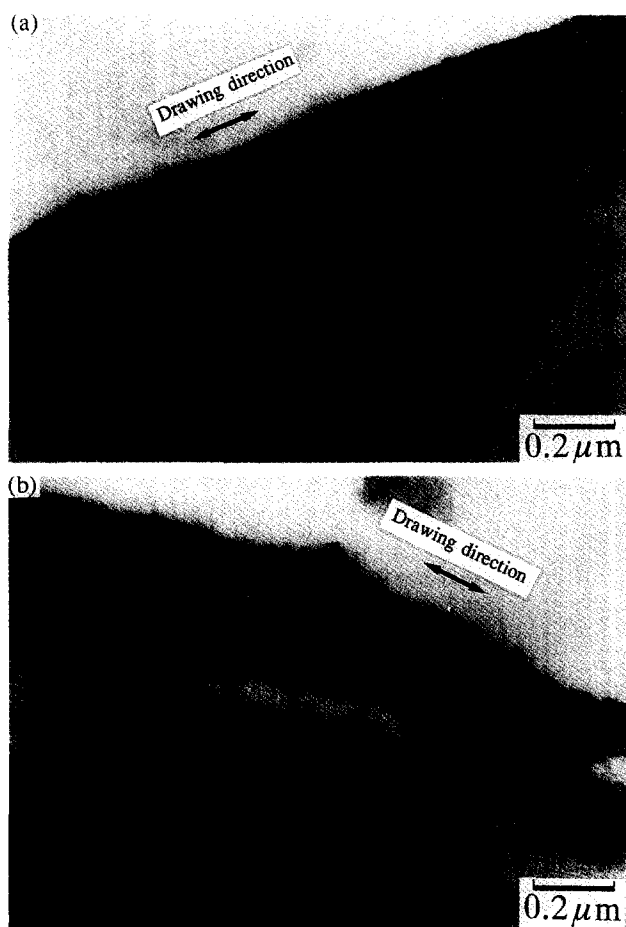


Figure 8 TEM photographs of the film drawn uniaxially up to a draw ratio of $\lambda = 3.5$ at a constant width and at 130°C: $T_{cr} = 20^\circ\text{C}$ (a) and 110°C (b)

remained in the film. These differences in morphology indicated that the film prepared at 20°C can deform more rapidly during drawing. This result agrees with the aforementioned result of the X-ray diffraction and also explains the higher stress after the yield point for the film prepared at 20°C in which microfibril deformation could occur at a relatively lower draw ratio.

Mechanism of micropore formation

All of the above data revealed that the stability of the β crystals has a dramatic correspondence with micropore formation during the drawing of β -PP films. Assuming that micropore formation is due solely to volume contraction followed by $\beta \rightarrow \alpha$ transformation, the total pore volume would be $0.017\text{ cm}^3\text{ g}^{-1}$, which is calculated from the difference in density between the α (0.936 g cm^{-3}) and β (0.921 g cm^{-3}) crystals. However, the pore volumes of the drawn films were found to be $0.179\text{ cm}^3\text{ g}^{-1}$ and $0.893\text{ cm}^3\text{ g}^{-1}$ for the films prepared at $T_{cr} = 20$ and 110°C respectively, when uniaxially drawn at a constant width (see Table 2). Therefore, pore formation is due not only to volume contraction accompanied by $\beta \rightarrow \alpha$ crystal transformation, but also to the deformation process of β -PP films.

There have been several models proposed for the deformation of semicrystalline polymers. According to Peterlin⁶, there may exist two deformation processes, i.e. the transformation of spherulite into fibrillar structure and the further deformation of the fibrillar structure. The

first mode seems to predominate at the early stage of drawing and is practically complete at a draw ratio below 10, while the second mode starts at a draw ratio around 2 and continues up to final fracture. In the deformation of β -PP, the former process ought to have a correspondence with phase transformation and micropore formation, because the increase in porosity was found to level off above a draw ratio of 2.5¹. As described earlier³, only the β crystals with the c axis parallel to the drawing direction are first subject to higher strain and stress to undergo the phase transformation. At a draw ratio above 2.5, a high stress is exerted on the β crystals with the c axis inclined with the drawing direction, and their lamellae were separated and rotated, inducing further phase transformation, fibril orientation and pore enlargement. These facts combined suggest that initial micropore formation mostly takes place at the early stage of drawing with deformation of the spherulite to microfibril transformation.

Kobayashi⁷, on the other hand, suggested a molecular view on the polymer deformation that the polymer chains in the original crystals are completely unfolded and subsequently recrystallized into c -axis-oriented crystals during the deformation. This model is not suitable to explain micropore formation in the drawn β -PP film as high as 40% in porosity. Petermann *et al.*⁸ proposed a similar but slightly different mechanism in which the chain segments within a narrow region of a few nanometres are unfolded and reorganized. This mechanism of a local melting/recrystallization process may lie somewhere between those of Peterlin and Kobayashi. Observing the rotation of the lamellae during the deformation of β -PP, Fujiwara *et al.*^{9–11} concluded that β crystal transformation goes through in the Petermann model. Based on our results, however, several different aspects should be added to these models.

Considering the deformation of β -PP, which involves both phase transformation and micropore formation, we postulate a mosaic model of β -PP consisting of lamellar blocks surrounded by weak boundaries. On drawing, the relatively weak boundaries between the lamellar blocks are first broken to form small pores, as indicated in Figure 7. If the β crystals are not stable, the deformational work is sufficient for partial melting of the lamellar blocks to induce phase transformation without enlarging the pores. If the β crystals are stable enough, they are allowed to rotate and separate from each other to increase the pore size. Therefore, the pore size is related to the size of lamellar block. Since the dimension of the lamellar blocks increases with increasing crystallization temperature, the more highly ordered β crystals formed at a higher T_{cr} can afford larger lamellar blocks and result in a larger pore size and a higher porosity. This mosaic model of β -PP is also consistent with the unusual mechanical properties of β -PP films. In particular, the lower Young's modulus and yield strength for the film prepared at higher T_{cr} should be attributed to the deformation of the larger weak boundaries formed between the larger lamellar blocks.

Since the phase transformation should involve a molecular chain rearrangement or even the change in the helix sense, its occurrence should be difficult under a weak stress. Therefore, the viscoelastic behaviour of the β -PP did not change below its melting point. In the case of the film prepared at lower T_{cr} , the thermal chain

rearrangement in the unstable β crystals was activated at relatively lower temperature, through the partial melting/recrystallization process to induce the phase transformation. Contrarily, the hindered mobility of the molecular chains in the stable β crystals formed at higher T_{cr} allowed the phase transformation at higher melting temperature.

In conclusion, crystal transformation and micropore formation were found to depend strongly on the stability of the β crystals in the β -PP film. The initial micropores are formed in the weak boundaries between lamellar blocks. In the boundaries, the deformation is initiated at the yield point of the film. If the lamellar blocks are continuously deformed with the $\beta \rightarrow \alpha$ transformation, the pore size does not increase much. If the β crystals are stable and resist the crystal transformation by reorganization of molecular chain and fibril formation, the stretching stress would concentrate on the boundaries of pores and enlarge the pores much more than expected from the volume contraction due to the phase transformation. Therefore, the porosity of the drawn film has a strong relationship with the lamellar size, which can be controlled by changing T_{cr} and T_{dr} .

ACKNOWLEDGEMENTS

The authors are indebted to Dr Akira Mochizuki

(Terumo Ltd, Japan) for his assistance in the porosity measurement and useful discussions. Dr Takashi Ito and Mr Hajime Tsuchiya (Kyoto Institute of Technology, Kyoto, Japan) are also greatly acknowledged for their TEM measurements.

REFERENCES

- 1 Chu, F., Yamaoka, T., Ide, H. and Kimura, Y. *Polymer* 1994, **16**, 3442
- 2 Turner-Jones, A., Aizlewood, Z. M. and Beckelt, D. R. *Makromol. Chem.* 1964, **75**, 134
- 3 Shi, G., Chu, F., Zhou, G. and Han, Z. *Makromol. Chem.* 1989, **190**, 907
- 4 Ikeda, N., Yoshimura, M., Mizoguchi, K., Kitagawa, H. and Kawashima, M. Japan Kokai H5-262936, 1993
- 5 Gregg, S. J. and Sing, K. S. W. 'Adsorption, Surface Area and Porosity', Academic Press, London, 1967, p. 195
- 6 Peterlin, A. *Colloid Polym. Sci.* 1975, **253**, 809
- 7 Kobayashi, K., cited in Geil, P. H., 'Polymer Single Crystals', Wiley, New York, 1963, p. 473
- 8 Petermann, J., Kluge, W. and Gleiter, H. *J. Polym. Sci., Polym. Phys. Edn* 1979, **17**, 1043
- 9 Asano, T. and Fujiwara, Y. *Polymer* 1978, **19**, 99
- 10 Asano, T., Fujiwara, Y. and Yoshida, T. *Polym. J.* 1979, **11**, 383
- 11 Yoshida, T., Fujiwara, Y. and Asano, T. *Polymer* 1983, **24**, 925